PORTI

OF T

DOCUM

ARE

ILLEGI

LA-UR -81-1364

TITLE: NEW LIQUID SCINTILLATORS FOR FIBER-OPTIC APPLICATIONS

MASTER

AUTHOR(S): S.S. Lutz, L.A. Franks, and J.M. Flournoy
EG&G, SBO

P.B. Lyons, P-14

SUBMITTED TO: SPIE Publication of Los Alamos Conf. on Optics
April, 1981

By acceptance of this article, the publisher recognizes that the U.S. Government retains a nonexclusive, royalty-free license to publish or reproduce the published form of this contribution, or to allow others to do so, for U.S. Government purposes

The Los Alamos Scientific Laboratory requests that the publisher identify this article as work performed under the auspices of the U.S. Department of Energy

University of California

LOS ALAMOS SCIENTIFIC LABORATORY
Post Office Box 1663 Los Alamos, New Mexico 87545
An Affirmative Action/Equal Opportunity Employer

DISTRIBUTION OF THIS DOCUMENT IS UNLIMITED

DISCLAIMER

Form No. 836 R3
St. No. 2629
12/78

UNITED STATES
DEPARTMENT OF ENERGY
CONTRACT W-7405-ENG. 36

A306

New liquid scintillators for fiber-optic applications*

S.S. Lutz, L.A. Franks, and J.M. Flournoy

EG&G, Santa Barbara Operations
130 Robin Hill Road, Goleta, California 93117

P.B. Lyons

Los Alamos National Laboratory
P.O. Box 1663, Los Alamos, New Mexico 87544

Abstract

New long-wavelength-emitting, high-speed, liquid scintillators have been developed and tailored specifically for plasma diagnostic experiments employing fiber optics. These scintillators offer significant advantages over commercially available plastic scintillators in terms of sensitivity and bandwidth.

FWHM response times as fast as 350 ps have been measured. Emission spectra, time response data, and relative sensitivity information are presented.

Introduction

Low-loss optical fibers are finding increasing application in plasma diagnostics, particularly when wide bandwidth and immunity to electromagnetic interference are required. The fibers normally serve to transmit a light pulse, generated in a radiation-to-light converter, to a remote photodetector. For the detection of high-energy electrons or gamma radiation, the Cerenkov light generated in the fiber itself is often sufficient for characterization of the radiation environment. For neutron detection, organic scintillators (liquid or plastic) are used because of their high neutron cross-sections.[1]

The efficiency of quartz fibers for signal transmission depends very strongly on wavelength. The optical attenuation due to Rayleigh scattering varies approximately as λ^{-4}. Material dispersion, which describes the variation in transmission time for signals of different wavelengths, varies approximately as $\lambda^{-1.7}$.

Modal dispersion, the variation of the propagation time for different fiber modes, is also wavelength dependent. Fibers are currently available with modal bandwidths in excess of one GHz-km at 850 nm. This can decrease to below 200 MHz-km at 600 nm. Long wavelength emission and short decay time in the transducer are thus central to optimal performance. While the exact scintillator parameters are dictated by the application, the minimum specification seems to be 660 nm emission, a FWHM (to a delta function input) of 2 ns, and a conversion efficiency comparable to conventional blue plastic scintillators. While progress has been made in developing such scintillators, an optimized scintillator for fibers has been unavailable.

Experimental procedures

The temporal and efficiency measurements were carried out on an electron linear accelerator (linac) and associated data acquisition systems. The samples were irradiated with 50-ns bursts of 6-MeV electrons at 60 ppm. The solutions were contained in 1-cm Suprasil spectrophotometer cells. The fluorescent emission was collected by a 3-m length of 1-mm diameter optical fiber. The fiber was coupled to a scanning monochromator and viewed by a microchannel plate (MCP) photomultiplier tube (PMT). An ITT FOP type F4129 was used in all cases except that of Figure 1, c in Table 1. The fast response of this scintillator necessitated the use of a Meritex LP-2.1D' MCP PMT. The system impulse response parameters with these two PMTs are given in Table 1, lines 9 and 10. The PMT output was then recorded using an HP nanosecond oscilloscope, which was interfaced to a data acquisition system, and allowed one to digitize the data, signal average, and do some analysis. The electron beam current

---

*This work was performed under the auspices of the U.S. Department of Energy under Contract No. DE-AC08-76DP00184. EG&G. By acceptance of this article, the publisher and/or recipient acknowledges the U.S. Government's right to retain a nonexclusive royalty-free license in and to any copyright covering this paper.

Reference to a company or product name does not imply approval or recommendation of the product by the U.S. Department of Energy to the exclusion of others that may be suitable.

A306

Table 1. Scintillator Emission Parameters (See Appendix A for Glossary of Chemical Terms and Abbreviations)

Fluor Number	Base	Shifter	Concentration (M)	Final	Concentration (M)	RT (ns)	FWHM (ns)	1/e (ns)	IPT (ns)	ε_{PK}	ϕ	λ (nm)
1	PVT			NE108		3.6	18.1	13.1	28.6	1.0	1.0	570
2	PVT			NE102		0.9	2.9	2.3	6.6	10.4	0.5	420
3	PVT			NE111		0.3	1.9	1.8	3.9	5.1	0.25	390
4	PC	PBD	2.7×10^{-3}	TPB	2.20×10^{-3}	0.4	1.3	1.0	2.6	4.0	0.14	450
5	PC	BIBUQ	15.0×10^{-3}	C-540A	1.00×10^{-1}	0.5	1.7	1.5	4.2	2.2	0.07	510
6	PC	BIBUQ	15.0×10^{-3}	C-540A	3.30×10^{-1}	0.15	0.36	0.4	2.5	1.7	0.03	518
7	BD	C-480	1.2×10^{-1}	#14567	1.25×10^{-2}	0.05	1.41	1.2	3.4	1.4	0.07	610
8	BA	C-480	1.6×10^{-1}	#14567	5.00×10^{-2}	0.5	1.2	1.2	2.7	1.0	0.05	650
9	Varian MCP #2210					0.14	0.21	0.10	0.25			
10	ITT MCP #F4129					0.27	0.49	0.20	0.61			

was monitored with a faraday cup placed behind the scintillator. Relative efficiency comparisons between scintillators were made by comparing the ratios of the digitized PMT output divided by the electron dose. NE108 was employed as a laboratory standard and was measured at the start of each day. The wavelength dependence of the PMT-fiber system response was determined by irradiating the fiber itself and wavelength-scanning the resulting cerenkov emission. The Cerenkov intensity is known to vary as λ^{-3}.[5]

Scintillators

Table 1 shows the emission parameters for a variety of scintillators when irradiated with 50-ps electron pulses. Column 1 is the scintillator solvent or base plastic, and columns 2 to 5 show the solutes and their concentrations. (See Appendix A for a glossary of chemical terms and abbreviations.) Columns 6 through 8 show the pulse rise time, FWHM, and 0.7-to 0.7/e decay times. The 0.7-to 0.7/e time approximates the lifetime for the decaying part of the pulse. Column 9 shows the 10. to 90% rise time of the integral (IPT) of the fluorescent impulses. For a gaussian function this parameter is related to the half power (-3 db) bandwidth by the expression:

$$BW\ (Hz) \times IPT\ (sec) = 0.35 \qquad (1)$$

Column 10, ε_{pk}, compares the amplitude of the peak of the impulse response, measured through a 10-nm spectral bandpass filter centered on the peak of the emission band, with the amplitude of NE108, measured at its peak of 570 nm. In column 11, ϕ is the ratio of the total amount of light emitted from each scintillator to the total NE108 emission. These numbers are obtained by multiplying the integrals of the impulse response waveforms by the integrals of the corresponding normalized, wavelength-calibrated emission spectra; they represent the total prompt emission. The integration times vary from 5 to 100 ns, depending upon the sweep speed setting on the sampling oscilloscope. Both ε_{pk} and ϕ depend on sample geometry. In this work the samples were 1 cm thick, and may exhibited some optical self-absorption in the short wavelength part of the emission band. In some cases, rather large corrections were made for a loss in system sensitivity in the red and blue ends of the visible spectrum. The surfaces of the plastic fluors were polished but otherwise were not treated in any special way. Because of these factors, the errors in ε_{pk} and ϕ are estimated to be 20-25%. Column 12 shows the fluorescent emission maxima.

Fluors 1, 2, and 3, Table 1, describe three commercially available plastic scintillators.[7] Fluor No. 1 is the slow blue light orange scintillator, NE108, which has an extremely wide emission spectrum, extending from 450 nm to over 700 nm. The FWHM impulse response varies from several nanoseconds at the blue edge of the emission band to near 20 ns at the red edge.

The emission parameters for NE102, fluor No. 2, are in good agreement with measurements published by Lyons and Stevens,[8] using high-energy electrons. Different results have been reported by other investigators using alternative excitation methods.[9,10]

Efficiency and response time for NE111, fluor No. 3, have been observed to vary from specimen to specimen. We have measured commercial products with FWHM response times as fast as 1.3 ns and as slow as 2.3 ns. We have attempted to give the pulse parameters for a representative sample. The emission spectrum of NE111 is given in Figure 1.

A306

Liquid "A", fluor No. 4, has been successfully used in a plasma-imaging experiment fielded at the Nevada Test Site.[1] This experiment utilized approximately 100 channels of graded-index fiber, each 550 m long, to relay space and time information to up-hole detectors. The peak of the emission spectrum for Liquid "A", given in Figure 1, is shifted from 450 nm to 540 nm when folded with the absorption spectrum of 500 m of fiber.

Fluor No. 5 is a two-solute system consisting of a blue-emitting wavelength-shifter, BIBUQ, and a green-emitting final solute, Coumarin 540-A (C-540A) dissolved in psuedo-cumene. This scintillator has a slow decay component that is predominant at the red edge of the C-540A emission band. The integral rise time, 4.2 ns at 510 nm, increases to nearly 20 ns at 600 nm. At high C-540A concentrations (fluor No. 6) the FWHM of this two-solute system becomes very fast (<360 ps), but the slow component is still present (IRT >2.6 ns). The emission spectrum of fluor No. 5 is given in Figure 1. A plot of the impulse response of fluor No. 6 is given in Figure 2.

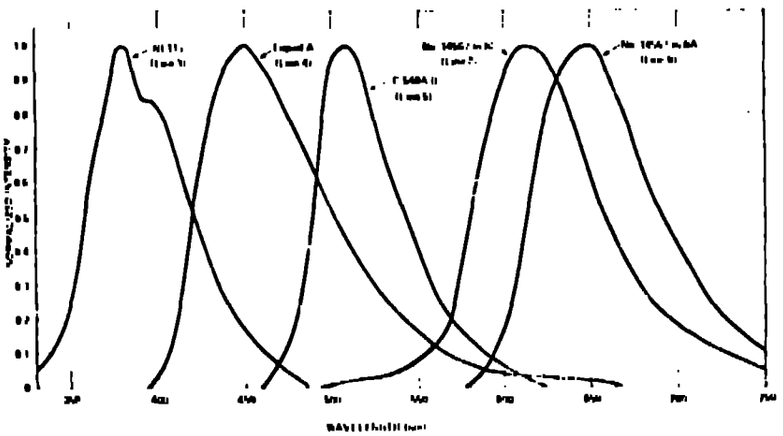

Figure 1. Scintillator emission spectra

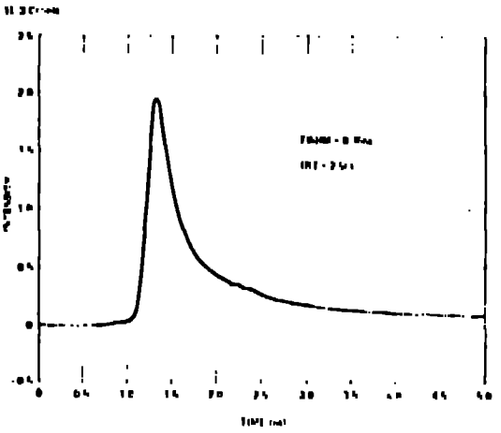

Figure 2. Impulse response of fluor No. 6

Fluors Nos. 7 and 8 are two red-emitting scintillators utilizing Kodak Dye #14567 as a final solute. Coumarin 480 is used as a wavelength-shifter. These dyes are dissolved in benzo-dioxane (BD, fluor No. 7) and benzyl alcohol (BA, fluor No. 8). The emission maximum of Kodak Dye #14567 varies from 510 nm, when dissolved in the non-polar solvent, psuedo-cumene, to 650 nm when dissolved in the very polar benzyl alcohol. The BD fluor is the more efficient of the two, but it also has the slowest integral rise time. The BA fluor has the larger emission wavelength, but it is the less efficient of the two scintillators using dye #14567. The emission spectra of fluors Nos. 7 and 8 are given in Figure 1.

Fluors and fibers

Fluor-fiber system designs involve a variety of engineering tradeoffs to achieve specified performance goals. Figure 3 illustrates such a tradeoff study in which absolute system sensitivity was investigated as a function of fiber length for several fluors. In this case, the system bandwidth was fixed (at 80 MHz), as was fiber type (high-quality graded-index) and photoreceiver (PTT type MA-3 photocathode; see Inset, Figure 3). The system sensitivity, S(L), in photoelectrons (pe) from the receiver photocathode per rad (100 ergs/g) deposited in the fluor is given by:

$$S(L) = K \cdot R(\lambda_0) \cdot T(\lambda_0, L) \cdot F(\lambda_0, L, BW) \qquad (2)$$

where

K = experimental calibration factor to express the sensitivity in absolute terms of photoelectrons per rad (see Appendix B)

$R(\lambda_0)$ = spectral sensitivity of PMT photocathode at the wavelength λ_0 (C/J)

$T(\lambda_0, L)$ = spectral transmission of the fiber of length L at the wavelength λ_0 (dimensionless)

and $F(\lambda_0, L, BW)$ = dimensionless fluor emission factor given by.

A306

$$F(\lambda_o, L, BW) = \frac{\Phi \cdot \int_{\lambda_o - \Delta\lambda/2}^{\lambda_o + \Delta\lambda/2} Em(\lambda)\, d\lambda}{\int_0^{\infty} Em(\lambda)\, d\lambda} \tag{3}$$

where

Φ = total relative total emission from the fluor (Table 1, column 11), (dimensionless)

$Em(\lambda)$ = normalized spectral emission of the fluor (Figure 1)

The center wavelength, λ_o, is selected at the peak of the fold of fluor emission, fiber transmission, and photocathode response versus wavelength. Figure 4 shows the result of this fold for Liquid "A" for several fiber lengths. As seen in the figure, λ_o shifts from 450 to 540 nm as the fiber length increases from 10 m to 1 km.

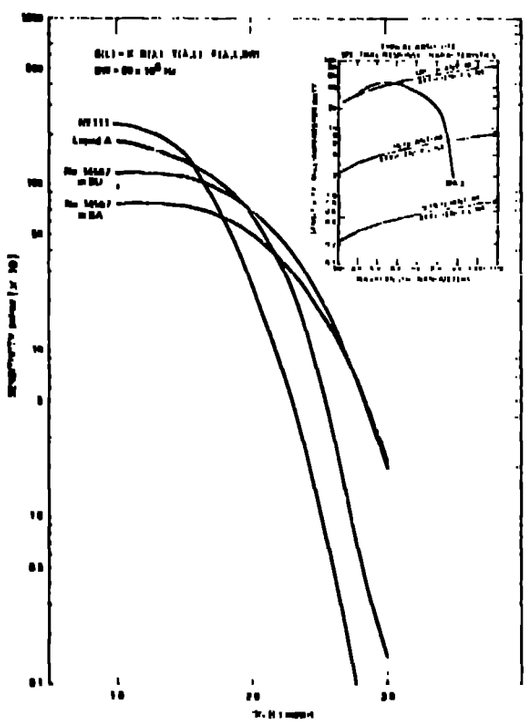

Figure 3. Fluor-fiber-PMT system sensitivity versus fiber length

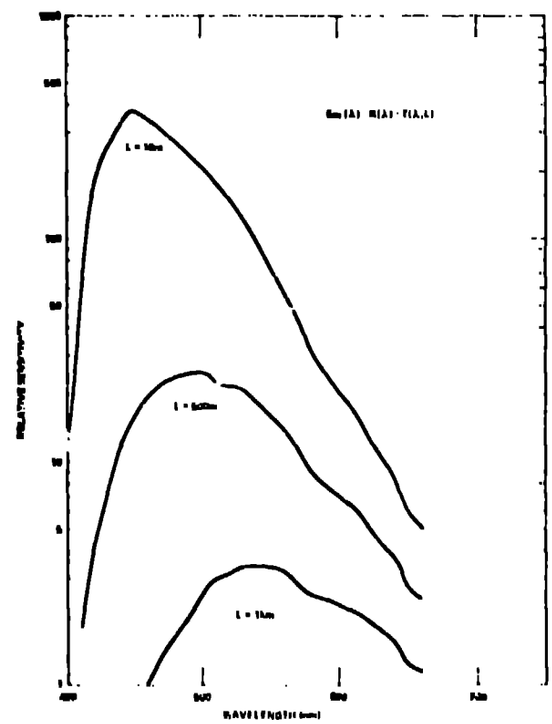

Figure 4. Liquid "A" emission spectrum folded with PMT and fiber

The optical bandpass, $\Delta\lambda$, is chosen to satisfy the system bandwidth (BW) criterion by:

$$\Delta\lambda = \frac{\sqrt{(0.35)^2 - (PW \cdot IRF)^2}}{M(\lambda_o) \cdot L \cdot BW} \tag{4}$$

where

$M(\lambda_o)$ = material dispersion of the fiber (s/nm-km)

L = length of fiber (km), and

BW = system bandwidth (s^{-1})

A306

As defined before, the integral rise time, IRT, is the 10%-90% rise time of the integral of the fluor response to a delta-function excitation, or simply the 10%-90% response to a step-function. For Figure 3, the bandwidth was set at 80 MHz, or

$$BW = 80 \times 10^{6}\ s^{-1} \tag{5}$$

The material dispersion of the graded-index fiber assumed here has been measured to be about 575 ps/nm-km at 500 nm wavelength, hence:

$$M(\lambda) = 575 \times 10^{-12} \cdot \left(\frac{500}{\lambda, nm}\right)^{3.3}\ s/nm\text{-}km \tag{6}$$

For applications requiring medium length fibers (10 m < L < 75 m) sensitivities of up to nine times larger than those shown in Figure 3 can be realized by switching from graded-index fibers to the new large numerical aperature (NA) "fat" fibers.*[1] For very short lengths (L < 10 m), single plastic-clad-silica (PCS) fibers up to 1-mm core diameter could be considered.[1] One-mm PCS fiber could provide sensitivities approximately 900 times larger than shown in Figure 3. However, modal dispersion from PCS fibers can exceed 150 ps/m over short lengths, so bandwidth may be a concern. In addition, the optical bandpass filter can be completely removed for short lengths (L < 100 m at 650 nm, or L < 20 m at 400 nm), which would result in a factor of two improvement over the numbers presented.

The top curve on the left of Figure 3 shows the sensitivity of an NE111 fiber system as a function of fiber length. For lengths less than 30 m, NE111 is the best of the four scintillators. The initially steeper slope of the NE111 curve is partly due to the increasing material dispersion at short wavelengths, and partly due to the large contribution of the scintillator IRT to the system bandwidth. Both effects cause A_ν to decrease rapidly with fiber length.

The next curve down of the left side of Figure 3 represents Liquid "A" (Table 1, line 4). The shorter IRT and longer wavelength emission of this scintillator, compared with NE111, means a larger A_ν at a given fiber length and system bandwidth. At L = 100 m, one is able to use over 55% of the entire emission band of Liquid "A" and still maintain the desired system bandwidth. With NE111, only 22% of the emission band is contained within a A_ν corresponding to a 80-MHz system. These rejected photons may be recovered by using a spectral equalizer;[1] however, for our calculation a blocking filter has been assumed. The bottom two curves on the left of Figure 3 show Kodak Dye #14567 dissolved in BA and BD. These fluors, because of their long wavelength emission, make a more sensitive system when utilized with fibers longer than 100 m. Dye #14567 in BD is the better of the two for an 80-MHz system.

These calculations can be extremely sensitive to changes in bandwidth. Figure 5 shows another calculation where the desired system bandwidth was set to 100 MHz. In this case, only Liquid "A" and Kodak Dye #14567 in BA and BD are considered, since NE111 is less than a 100-MHz scintillator. In this calculation, Dye #14567 makes a less sensitive scintillator when dissolved in BD than when dissolved in BA. This is because of the relatively slow IRT of the BD scintillator (3.4 versus 2.7 ns).

Linearity

We have not considered scintillator linearity in this presentation. When system sensitivities fall below 30 photoelectrons/rad, peak dose rates in excess of 10^{10} rad/s are required to obtain statistically meaningful signals. This laboratory has documented the linearity of only three of the scintillators presented: NE111, SF108, and Liquid "A". NE111 and Liquid "A" have been measured to be linear at doses rates up to 10^{12} rad/sec. On the other hand, NE102 has been observed to go nonlinear when exposed to dose rates exceeding 3×10^{10} rad/sec.[2] Linearity may be a problem with the experimental scintillators. Measurements to determine their saturation limits will be done in the near future.

Conclusions

The new long-wavelength scintillator formulations presented here represent significant improvements in system sensitivity and bandwidth for applications requiring long optical fibers. The best choice of a scintillator depends on fiber length; currently available blue scintillators are still the best choice for short fiber runs. Linearity of the redder scintillators needs further investigation.

---

*"Fat" fiber diam 100 mm, NA 0.3, bandwidth 20 GHz-km at 850 nm

A306

References

1. "Utilization of Fiber Optics in Radiation Diagnostics," P.B. Lyons, et al, Fiber Optics and Communications Exposition, Chicago, Illinois, Los Alamos National Laboratory Report LA-UR-78-1866 (September 1978).
2. "The Development of Fast Liquid Scintillators for Fiber Optic Applications," P.B. Lyons, L.A. Franks, and S. Lutz, Liquid Scintillation Counting and Recent Development, Vol. 2, Acad. Press, C.I. Peng and D.L. Horrocks, editors, 1980.
3. ITT, Fort Wayne, Indiana.
4. Varian LSE, Palo Alto, California.
5. "Cerenkov Radiation and Its Applications," J.V. Jelly, Pergammon Press (1958).
6. Nuclear Enterprises, San Carlos, California.
7. P.B. Lyons and J. Stevens, Nucl. Instr. and Meth., 114, 313 (1974).
8. A.J. Campillo, R.C. Hyer, and S.H. Shapiro, Nuclear Inst. and Meth., 120, 533 (1974).
9. J.G. Pronko and L.F. Chase, "Temporal Characteristics and Saturation Effects of Organic Scintillators to Low Energy X-Rays," Nucl. Instr. and Meth., 164, 79-92 (1979).
10. Siecor Optical Cables, P.O. Box 489, Hickory, North Carolina.
11. Quartz Products Corporation, 688 Somerset Street, Plainfield, New Jersey.
12. "Signal Enhancement by Spectral Equalization of High Frequency Broadband Signals Transmitted Through Optical Fibers," J. Ogle and P.B. Lyons, Fiber Optics Conference, San Francisco, EG&G, Santa Barbara Operations No. S-158-TP (18 September 1980).
13. "LASL Support Program Project Summary July '80," EG&G Report No. EGG 1183-2405.
14. "Characterization of Three Fluors," EG&G Report No. EGG 1183-2376 (July 1978).

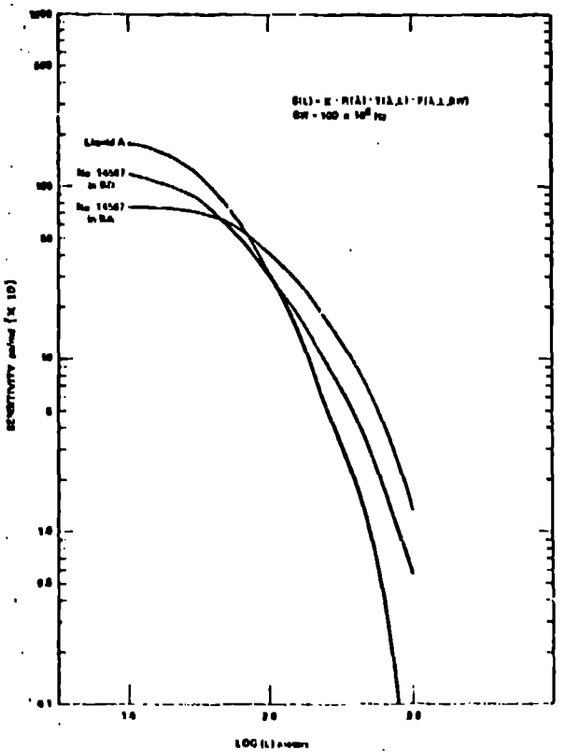

Figure 5. Fluor-fiber-PMT system sensitivity versus fiber length

Appendix A: Glossary

All chemicals and solvents in this work were used as received from the manufacturer, without further purification. The solutions were not outgassed.

Abbreviation	Supplier[a]	Chemical Name
BIBUQ	NEI	4-4"-Di(2-butyloctoxy-1)-p-quaterphenyl
C-480	Exciton	Coumarin 480 or Coumarin 120, 2,3,5,6-1H,4H, tetrahydro-8-methylquinolazino-(9,9a,1-gh)coumarin
C-540A	Exciton	Coumarin 540A, 1,4,5,3H,6H,1 OH, tetrahydro-8-trifluoromethyl(1)benzopyrano(9,9a,1-gh)
PBD	Exciton or NEI	2-phenyl-5-(4-biphenylyl)-1,3,4-oxadiazole
TPB	NEI or Aldrich	1,1,4,4-tetraphenylbutadiene
#14567	Kodak	4-dicyanomethylene-2-methyl-6-p-dimethylamino styryl-4H-pyran
AN	Aldrich	anisole
BA	Aldrich	benzyl alcohol
BD	Spectrum	benzodioxane
PC	NEI	pseudocumene (1,2,4-trimethylbenzene)

[a]Aldrich = Aldrich Chemical Co., Inc.
Exciton = Exciton Chemical Co., Inc.
Kodak = Eastman Kodak Co.
NEI = Nuclear Enterprises, Inc.
Spectrum = Spectrum Chemical Manufacturing Co.

A306

Appendix B: Calibration factor, K

The calibration factor, K, in Eq. (2) was derived from the following experiment. A 4-cm-thick volume of Liquid "A" was placed in a calibrated ^{60}Co gamma field. The fluor was viewed by a short length of PCS fiber, with a numerical aperture of 0.3, and 250-μm-diam core. A calibrated photodiode was used to measure the amount of fiber-transmitted fluorescent photon energy transmitted through a narrow band optical filter with a 10-nm bandpass centered at 540 nm. Correcting for filter transmission and photodiode sensitivity at 540 nm, one finds that the ratio of optical energy, in joules, incident on the photocathode to the gamma dose, in rads, to the fluor was 2×10^{-14} J/rad. For a system employing a fiber of numerical aperture NA, core diameter d μm, with a narrow-band filter of peak transmission T_{fp}, K is:

$$K = \frac{2 \times 10^{-14}\ \text{J/rad}}{1.6 \times 10^{-19}\ \text{C/electron}} \cdot \left(\frac{(\text{NA})\ d\ \mu\text{m}}{0.3\ (250\ \mu\text{m})}\right)^2 \cdot T_{fp} \cdot \frac{\int_0^\infty \text{Em}(\lambda)_{\text{Liquid "A"}}\, d\lambda}{4 \cdot \int_{535}^{545} \text{Lm}(\lambda)_{\text{Liquid "A"}}\, d\lambda}$$

$$= 3.75 \times 10^5\ \frac{\text{J-electron}}{\text{rad-C}}$$

For the "fat" fiber referred to with NA = 0.4, diam = 100 μm, the gain in light collection over the 0.2 NA 50-μ-diam graded-index fiber, which we assumed for purposes of developing the Figure 3 data, is:

$$\left(\frac{0.4 \times 100\ \mu\text{m}}{0.2 \times 50\ \mu\text{m}}\right)^2 = 4$$